Inertially-Driven Buckling and Overturning of Jets in a Hele-Shaw Cell

Adriana I. Pesci,[1] Martin A. Porter,[1] Raymond E. Goldstein[1,2]
Department of Physics[1] and Program in Applied Mathematics,[2] University of Arizona, Tucson, AZ 85721
(Dated: January 7, 2003)

We study fluid jets descending through stratified surroundings at finite Reynolds number in Hele-Shaw flow. This system displays rich dynamics: buckling and overturning of the jet, formation of a confining conduit of entrained fluid with smooth or unstable traveling waves. Leading-order corrections to Darcy's law for small Reynolds number are shown to yield a damped, forced Burgers equation for the interfacial vorticity which supports singularities depending upon initial conditions. These singularities correspond to the overturning and unstable waves seen in the experiments.

PACS numbers: 05.45.-a, 47.15.Gf, 47.20.Ft, 68.05.-n

Fluid flow between parallel plates, the classic geometry of Hele-Shaw cells, is often considered a quintessential low Reynolds number system [1]. Yet, in the laboratory it is straightforward to achieve a Reynolds number (Re) of order 1 with conventional fluids and relatively small plate spacings. This raises the interesting possibility of studying inertial effects in a controlled manner by varying the fluid viscosity, cell geometry, and external forcing. Indeed, Flekkoy, *et al.* [2] presented such results on hydrodynamic irreversibility by varying the velocity of a smoothly driven flow. A richer class of phenomena occurs when inertia itself is responsible for hydrodynamic instabilities in otherwise stable systems [3, 4].

Here we discuss the *buckling instability* of a gravity-driven jet in a Hele-Shaw setup. The buckling of fluid jets has a long history, starting from the work of Taylor [5] who emphasized connections between fluid mechanics and elasticity, to more recent work [6–8] concerning jets surrounded by air impacting on a surface. Unlike these systems, the dynamics of jets in our two-fluid setup is dominated by viscous shear, a situation that has had some theoretical attention. Lister [9] considered a gravity-driven fluid *sheet* descending through a uniform fluid of different viscosity, using a perturbation in Re on the Navier-Stokes equations. He concluded that at $\mathcal{O}(Re^0)$ small-amplitude excitations on a straight interface travel as waves, but at $\mathcal{O}(Re^1)$ an instability develops in the absence of surface tension. The mechanism of this instability is the feedback between the vorticity left in the wake of a traveling wave and the wave itself. In the problem of interest here, we study an analogous effect in Hele-Shaw flow *in the absence of surface tension* by experimental and theoretical means. On the experimental side, in analogy to three-dimensional studies of the dynamics of jets [10, 11], we consider a saline plume descending through a salinity gradient which causes it to decelerate gradually, and thereby buckle (see Fig. 1). As mentioned, there is no surface tension between the jet and surround because the only distinction between the two is the solute concentration. As the jet descends through the gradient and decelerates, mass conservation can be achieved by two competing mechanisms. At low flow rates, diffusion dominates advection and the jet loses solute to its surroundings and simply broadens. At high flow rates the jet has constant density and changes its profile by broadening or buckling. In the fully-developed buckled regime, the solute diffusion time is long compared to the characteristic time of the instability; the distinction between the fluids is persistent. The theory we discuss is a generalization of Darcy's law to include weak inertia, similar in spirit to those that account for non-Newtonian effects [12, 13]. We express our results compactly and systematically through coupled partial differential equations for the vortex sheet strength γ at the interface between the two fluids and the position of

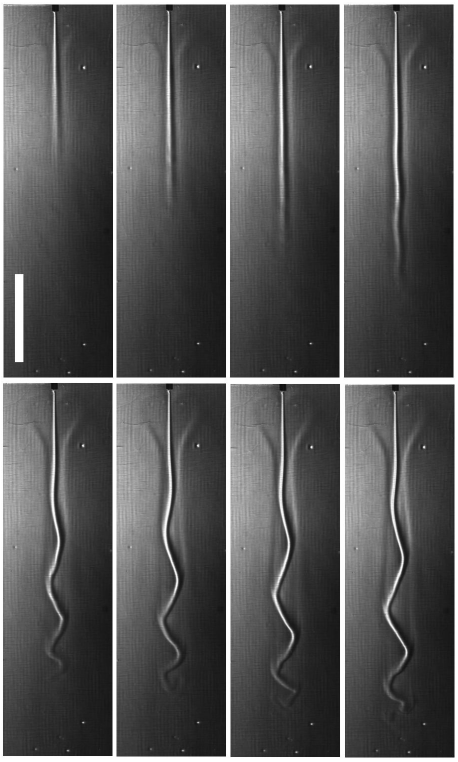

FIG. 1: A 1 M jet descending into a gradient $G = 0.04$ M/l-cm. at velocities from $0.02 - 0.18$ cm/sec. Scale is 1 cm.

the interface itself. This is analogous to models [14] of the Kelvin-Helmholtz instability of thin inviscid jets. The equation of motion for γ is a damped, forced Burgers' equation [15] which forms finite-time shocks for suitable initial conditions. These shocks correspond to overturning of the buckled jet and unstable growth of wavelike excitations observed experimentally (Figs. 2 and 3).

The only significant optical distinction between the jet and surrounding fluid is a small difference between their indices of refraction. This feature makes the flow patterns observable best with Schlieren imaging, which is sensitive to gradients of refractive index. Our Schlieren system is in the standard "Z" configuration [16] with the light source at the upper end, one mirror at each vertex (152.5 mm F/8 parabolic telescope mirrors), the chamber between them on the diagonal, and a ccd camera at the lower end. The light source is a bright LED focussed on a diffusing plate and passed through an iris; the video images were acquired from a digital ccd camera (Hamamatsu C7300) with a $80-200$mm zoom lens (Nikon), and recorded to a PC with a frame grabber (National Instruments) under computer control (Labview). A knife-edge at the focus of the second mirror achieves the Fourier filtering of Schlieren imaging [16].

The Hele-Shaw cell consists of two 30 cm $\times$ 30 cm polycarbonate sheets 12.7 mm thick, separated by a rubber gasket 3 mm thick, permanently glued and caulked to one plate, sealed with vacuum grease to the other, and held in place by an aluminum frame and a set of clamps. A 25 gauge needle with an interior diameter of 0.024 cm at the top of the chamber is the entry point for the jet. Two additional needles inserted through ports (Instech Labs, PMINP-SIL-C35) mounted in holes drilled in one of the plates at the bottom are the entry points for the fluid surround. The jet is forced into the chamber with a syringe pump [17] driving a gas-tight glass syringe (Hamilton). We shall use the average fluid velocity u at the needle associated with the controlled fluid fluxes as our experimental variable. These velocities range from $0.02-1$ cm/s. Solutions were made from RO purified water and reagent-grade NaCl (Sigma), with a diffusion constant of $D = 1.5 \times 10^{-5}$ cm^2/s [18]. Linear salinity gradients were produced by a variant of the well-known "two-bucket" method [19] in which the fluid flow was controlled by peristaltic pumps instead of driven purely by gravity. Typical gradients used in the experiments correspond to a variation of concentration from 1.0 M at the bottom to 0 M at the top, or a gradient G of 0.04 M/l-cm. This in turn implies a maximum variation in the index of refraction of about 0.01 [18]. A variety of jet concentrations between 1 and 2 M was investigated. The Reynolds number of the jet is naturally calculated as uw/ν, with w the jet diameter and $\nu = 0.01$ cm^2/s the kinematic viscosity of water. Using the values for u quoted above, Re is in the range of $0.03-3$.

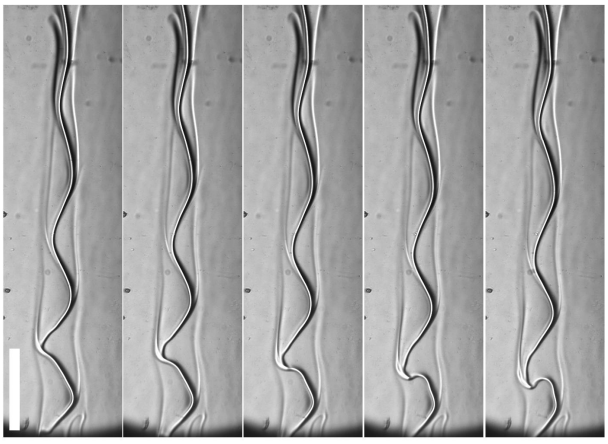

FIG. 2: Buckling and overturning of a jet descending through a gradient. Images are 0.66 sec apart; scale bar is 1 cm.

As shown in Figure 1, at low flow velocities the jet is straight, disappearing by diffusion at a termination length ℓ which increases with flow rate. For each gradient G and jet molarity J there is a critical velocity u_c above which the jet buckles and ℓ remains nearly constant. It is this buckling that allows for mass conservation. The density of the jet in this figure equals the fluid density at the *bottom* of the chamber, so the fact that it terminates after traversing only a small fraction of the depth of the gradient indicates that it loses density through diffusion. Solute diffusion across the width w of the jet occurs on a time scale $t_D \sim w^2/D \sim 170$ sec. On the other hand, at the lowest flow rates the advection time t_a for a fluid element to traverse the length $\ell \sim 2$ cm is $t_a \sim \ell/u \sim 100$ sec. Clearly, there is sufficient time for appreciable diffusive broadening to occur, as seen in the figure.

At all flow rates we find that the jet, whether straight or buckled, is traveling inside a *conduit* whose edges can be clearly seen in Figs. 1 and 2. Near the nozzle the conduit flares upward away from the jet, narrows to a minimum somewhat below the nozzle and then increases steadily downward. When the jet buckles its amplitude maxima always approach the edges of the conduit as they travel downward. By direct observation of the motion of tracer particles (10 μm hollow glass spheres, Potters Industries), we determined that the conduit consists of essentially fresh water that is viscously entrained from above by the downward moving jet to the point at which its buoyancy drives it upward as a flow along the conduit edge. It is interesting to note that the confinement of this recirculating flow in such a narrow conduit is strikingly different from the much broader backflow that occurs in the absence of a density gradient [11, 20, 21]. Indeed, the shape of the conduit itself is an important free boundary problem. Evidence for recirculation within the conduit can clearly be seen at large flow rates, when wavelike excitations ("*blips*") travel up the conduit edge [22, 23], as shown by the time series in Fig. 3. As these wave travel

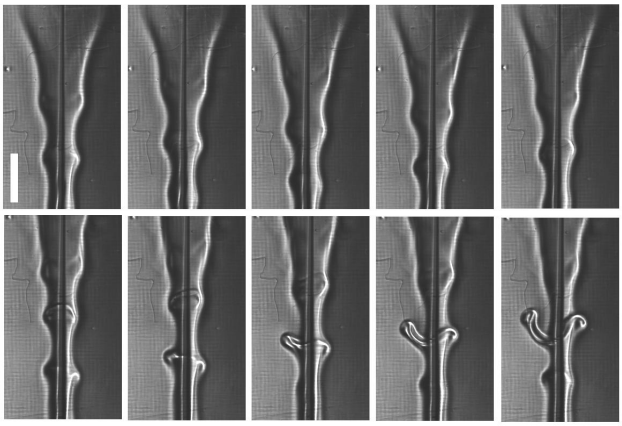

FIG. 3: Waves at the conduit edge. Upper sequence shows growth and subsequent decay; lower sequence shows unstable growth. Images are 0.8 s apart; scale bar is 0.5 cm.

upward they either transiently grow and then decay or continue to grow and eventually form a separate plume. There are corresponding "anti-blips" on the jet itself that travel downward and also may grow so large as to detach.

Beyond the critical velocity we see a classical bifurcation scenario, with the buckling amplitude as the natural order parameter, and the nozzle velocity u as the control parameter. Given that the amplitude varies down the gradient, we have chosen to record it (see Fig 4(a)) for the wave farthest from the nozzle, where the conduit width has saturated. The frequency ω and initial wavelength λ of the traveling waves are shown in Figs. 4(b) and (c) as a function of u for a particular gradient and jet density. The amplitude and frequency data are consistent with a supercritical Hopf bifurcation. Over a wide range of flow rates beyond u_c the jet maintains its thickness as it descends, and as it slows down the wavelength of buckling decreases while the amplitude increases. This is one obvious mechanism to conserve mass. This flaring is intrinsic to this system and very important, for it implies that the maximum slope of the jet always increases as it progresses downwards, and as a consequence, as seen clearly in Figure 2, the jet always overturns as it nears the termination point.

Given the experimental phenomena reported above in Hele-Shaw geometry and the range of Reynolds numbers at which they occur, it is natural to study modifications to Darcy's law for finite Re. Consider a Hele-Shaw cell of lateral dimensions $L \times L$, with plate spacing $d \ll L$, filled with fluids of common viscosity η. Assuming there exists a characteristic velocity U, we define anisotropic rescalings $\tilde{\mathbf{u}} = U\mathbf{v}$, $t = (L/U)\tau$, $x' = x/L$, $y' = y/L$, $z' = z/d$, where (x, y) are in-plane coordinates and z is perpendicular to the plates. Neglecting the component of $\mathbf{v}$ in the z-direction, and introducing the rescalings into

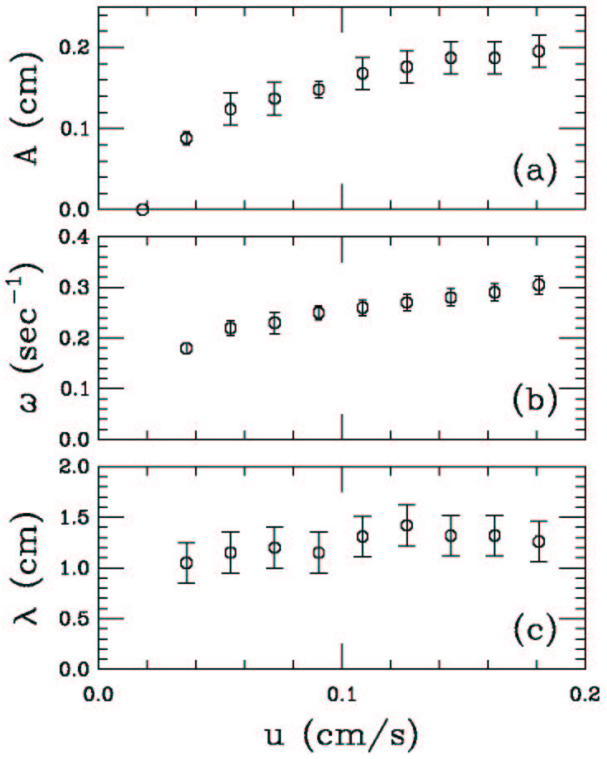

FIG. 4: Maximum buckling amplitude (a), frequency (b), and initial wavelength (c) as a function of flow rate for G=0.04 M/l-cm and $J = 1.0$ M.

the Navier-Stokes equation we obtain

$$Re\frac{d}{L}\left[\frac{\partial \mathbf{v}}{\partial \tau} + (\mathbf{v}\cdot\nabla')\,\mathbf{v}\right] = -\frac{d^2}{U\eta L}\nabla' p + \frac{\partial^2 \mathbf{v}}{\partial z'^2} \qquad (1)$$

where $\nabla' = (\partial/\partial x')\hat{\mathbf{x}} + (\partial/\partial y')\hat{\mathbf{y}}$ and $Re = \rho U d/\eta$.

We propose a series expansion of $\mathbf{v}$ in powers of Re of the form $\mathbf{v} = \mathbf{v_0} + Re\ \mathbf{v_1} + \mathcal{O}(Re^2)$. It is then a straightforward exercise to substitute into (1), solve for $\mathbf{v_0}$ and $\mathbf{v_1}$ subject to the usual stick boundary conditions at the plates, average over the z-coordinate, and then undo the original rescalings to obtain the averaged velocity $\mathbf{u}$ up to first order in Re

$$\mathbf{u} \;=\; \mathbf{u}_0 - Re\frac{d}{10U}\left[\frac{\partial \mathbf{u}_0}{\partial t} + \frac{3}{7}\mathbf{u}_0\cdot\nabla\mathbf{u}_0\right] + \mathcal{O}(Re^2, d^4) \qquad (2)$$

where $\mathbf{u}_0 = -(d^2/12\eta)\nabla p$. The entire velocity field can be recast in terms of the vortex sheet strength γ at the interface(s) Γ between the two fluids where $\gamma = \hat{\mathbf{t}}\cdot(\mathbf{u}_1 - \mathbf{u}_2)\,|_\Gamma$ [24, 25]. Expansion of γ as $\gamma_0 + Re\gamma_1 + \cdots$ and utilizing continuity of $\hat{\mathbf{n}}\cdot\mathbf{u}$ at Γ yields

$$\gamma + \frac{d^2}{10\nu}\left[\gamma_t + \frac{3}{7}\gamma\gamma_x\right] = \hat{\mathbf{t}}\cdot\nabla\Delta\mathbf{u}_0|_\Gamma\ . \qquad (3)$$

Consider a nearly straight interface between two fluids with density difference $\Delta\rho$ that varies linearly with vertical position x. Then the right-hand-side of (3) is proportional to $\Delta\rho(x)g$. For simplicity, we define the parameter

$\epsilon = dRe/10U$ and let $x' = (7x/3\epsilon)$ and $t' = (t/\epsilon)$, and thereby obtain a damped forced Burgers' equation,

$$\gamma_{t'} + \gamma\gamma_{x'} + \gamma = K - \alpha' x' \ , \tag{4}$$

where K and α represent a reference density difference and gradient. The nonlinearity is responsible for steepening the vorticity, while the standard contribution arising from Darcy's law (third term on the left-hand side) is responsible for damping it. Whereas in the inviscid Burgers' equation shocks form for generic initial conditions, the competing effects in the damped version allow for shocks to occur only if the initial condition satisfies a constraint. Solving Eq. (4) by the method of characteristics [14, 15], with $d\gamma/dt' = K - \alpha x' - \gamma$, $dx'/dt' = \gamma$, and initial condition $\gamma_0(x')$, after undoing the rescalings we find that constraint to be

$$\frac{d}{U}\gamma_x < -\frac{35}{3}\left(1 + \sqrt{1 - 4\alpha}\right)\frac{1}{Re} \ . \tag{5}$$

This results shows that a singularity will occur more readily for larger Reynolds numbers and will not occur in the strict limit of Darcy's law.

For thin fluid layers, such as the jet itself or the conduit, the dynamics of γ can be incorporated into an equation of motion of the interface(s) [26, 27]. For two interfaces whose displacements are reflection-symmetric about a midline (as in Fig. 3), one obtains a lubrication-type equation which at leading order in h becomes

$$h_t = -\left(h\gamma\right)_x \ . \tag{6}$$

As discussed by Pugh and Shelley [14], given suitable initial conditions, the coupled PDEs (4) and (6) can display an unbounded finite-time singularity for h or can simply relax to a traveling-wave with γ constant. This is consistent with the observations shown in Fig. 3, even though the unstable growth mode is not truly unbounded. This discrepancy stems from the limited domain of validity of the lubrication approximation.

For meandering displacements the leading-order interfacial equation of motion describes a wave,

$$h_t = -\gamma h_x \ , \tag{7}$$

and as such does not have the flux form of the lubrication dynamics (6). Here, the singularity in γ is inherited directly by h, which will become multivalued at a finite time. This is consistent with the overturning in Fig. 2.

We have presented a number of experimental observations concerning the rich dynamics of decelerated jets at finite Reynolds number, as well as some theoretical analysis that should serve as a starting point toward a more complete understanding. Among the important open problems are the detailed understanding of the conduit formation, shape, and dynamics, the stability analysis of a jet contained within such a conduit, the nonlinear feedback between the fully-buckled jet and the conduit, and the detailed understanding of the finite-time singularities associated with overturning jets and conduit waves.

We are grateful to Andrew Belmonte and Juan M. Restrepo for important discussions, to John O. Kessler for inspiring this work, and to the Santa Fe Institute for hospitality. This work was supported by NSF CTS0079725 and DMR9812526 and the Bridge Program.

[1] D. Bensimon, L. Kadanoff, S. Liang, B. Shraiman, and C. Tang, Rev. Mod. Phys. **58**, 977 (1986).
[2] E. Flekkoy, T. Rage, U. Oxaal, and J. Feder, Phys. Rev. Lett. **77**, 4170 (1996).
[3] P. Gondret and M. Rabaud, Phys. Fluids **9**, 3267 (1997).
[4] F. Plouraboué and E. Hinch, Phys. Fluids **14**, 922 (2002).
[5] G. Taylor, *Proc. 12th Intl. Congr. Appl. Mech.* (Springer-Verlag, 1969).
[6] B. Tchavdarov, A. Yarin, and S. Radev, J. Fluid Mech. **253**, 593 (1993).
[7] L. Mahadevan and J. Keller, Proc. R. Soc. A **452**, 1679 (1996).
[8] L. Mahadevan, W. Ryu, and A. Samuel, Nature **392**, 140 (1998).
[9] J. Lister, J. Fluid Mech. **175**, 413 (1987).
[10] J. Kessler, J. Fluid Mech. **173**, 191 (1986).
[11] C. Dombrowski et al., preprint (2003).
[12] L. Kondic, M. Shelley, and P. Palffy-Muhoray, Phys. Rev. Lett. **80**, 1433 (1998).
[13] E. Poire and M. Ben Amar, Phys. Rev. Lett. **81**, 2048 (1998).
[14] M. Pugh and M. Shelley, Comm. Pure Appl. Math. **51**, 733 (1998).
[15] G. Whitham, *Linear and Nonlinear Waves* (Wiley Interscience, 1974).
[16] D. Holder and R. North, *Schlieren Methods* (H.M. Stationery Off., 1963).
[17] Syringe pumps included a New Era N1000 and a custom device based on a DC servo motor with submicron resolution (Newport 850G/ESP100).
[18] R. Weast, ed., *CRC Handbook of Chemistry and Physics* (CRC Press, 1979).
[19] H. Berg, *Random Walks in Biology* (Princeton University Press, 1983).
[20] M. Smith, Phys. Fluids A **1**, 494 (1989).
[21] A. Pesci et al., preprint (2002).
[22] J. Whitehead and K. Helfrich, Nature **336**, 59 (1988).
[23] K. Helfrich and J. Whitehead, Geophys. Astrophys. Fluid Dynamics **51**, 35 (1990).
[24] G. Baker, D. Meiron, and S. Orszag, J. Fluid Mech. **123**, 477 (1982).
[25] G. Tryggvason and H. Aref, J. Fluid Mech. **136**, 1 (1983).
[26] T. Hou, J. Lowengrub, and M. Shelley, J. Comp. Phys. **169**, 302 (2001).
[27] R. Goldstein, A. Pesci, and M. Shelley, Phys. Fluids **10**, 2701 (1998), and references therein.